A Review of Frequency Domain Methods for Fatigue and Damage Estimation

Pierre Lague

[1] Inria, Rennes (France)

June 5, 2026

Abstract

The prediction of fatigue life under random vibration loading is a central challenge in the design and assessment of mechanical structures. While time-domain methods such as rainflow counting remain the established reference, they require long-duration time histories and incur significant computational cost. Frequency-domain approaches, in contrast, enable efficient estimation of stress-range probability distributions and fatigue damage directly from spectral representations of the excitation and structural response. This paper presents a comprehensive review of the principal spectral methods developed for vibration-fatigue assessment. Beginning with classical formulations such as Rice's narrow-band model and its subsequent wide-band corrections—Wirsching–Light, the $\alpha_{0.75}$ rule, Jiao–Moan, Gao–Moan, and Zhao–Baker—the review highlights their underlying assumptions, theoretical foundations, and known limitations. Particular attention is given to the Dirlik and Tovo–Benasciutti models, which remain the most accurate and widely adopted techniques for estimating stress-range distributions in practical engineering contexts.

In addition to surveying the theoretical background—including Gaussian random processes, spectral moments, transfer functions, and S–N fatigue behavior—the paper provides a structured workflow for integrating frequency-domain methods into real-world engineering analyses. This includes vibration measurement, stress reconstruction via frequency response functions, PSD characterization, material modeling, and fatigue-damage accumulation using Miner's rule. The discussion emphasizes both the computational benefits and the applicability boundaries of spectral methods, especially in relation to non-Gaussianity, non-stationarity, and complex loading conditions.

Overall, this review consolidates the theoretical developments, practical methodologies, and comparative insights necessary for selecting and applying frequency-domain fatigue techniques. It establishes a coherent foundation for subsequent research within this PhD project, particularly regarding improved modeling strategies and the advancement of spectral approaches for modern vibration-fatigue applications.

1 Introduction

Engineering structures operating in real-world environments—wind turbines, aircraft, satellites, rotating machinery, bridges, and military vehicles—are frequently subjected to unpredictable, continuously fluctuating vibrational loads. These random vibrations, induced by wind turbulence, aeroacoustic noise, seismic activity, or operational conditions, do not follow simple periodic patterns. Instead, they are characterized by variable-amplitude loads with no measurable periodicity [1].

The consequence of prolonged exposure to such random vibrations is cumulative fatigue damage: repeated, varying stress cycles gradually initiate and propagate microscopic cracks within materials, ultimately leading to structural failure [2]. Fatigue remains one of the most prevalent and costly failure modes in mechanical engineering. Offshore wind turbines, for example, experience premature bearing failures—far earlier than design life predictions—resulting in expensive maintenance, crane mobilization, and production loss. Similarly, aircraft structural components and military vehicle frames accumulate fatigue damage under operational vibration environments, making accurate assessment essential for design validation and predictive maintenance strategies.

Traditionally, engineers estimate fatigue damage using time-domain methods: synthesizing long stress time-histories from measured or specified vibrations, extracting cycles using the rainflow counting algorithm [2], and

summing damage according to the Palmgren-Miner hypothesis [3, 4]. This approach is conceptually intuitive, thoroughly validated, and avoids restrictive assumptions about the nature of the random process [5–8].

However, time-domain analysis demands substantial computational resources. Accurate fatigue estimation requires very long time records—often spanning hours or days of simulated data—to capture the statistical characteristics of random processes adequately. For structures analyzed using finite element (FE) methods, where each time-step integration is computationally expensive, this becomes prohibitive [5]. In iterative design processes or real-time condition monitoring systems where many analyses must be performed rapidly, the computational burden escalates dramatically [9].

Frequency-domain (spectral) methods represent a fundamentally different approach: they calculate fatigue damage directly from spectral properties—specifically the power spectral density (PSD) and its statistical moments—without generating time histories [10, 11]. Random loads observed in real-world scenarios can be viewed as realizations of stationary Gaussian processes naturally described in the frequency domain by their PSD. By assuming stationarity, Gaussianity, and linear damage accumulation (Palmgren-Miner rule), spectral methods provide closed-form or semi-analytical expressions for fatigue damage rate.

1.1 Objectives and Structure

Despite their significant advantages, frequency-domain spectral methods remain less widely understood in engineering practice than traditional time-domain approaches. The diversity of available models—each based on different assumptions, theoretical foundations, and ranges of validity—makes the selection of an appropriate method far from straightforward.

To address this gap, this paper provides a structured and pedagogical introduction to vibration-fatigue estimation in the frequency domain. The presentation follows a complete end-to-end pipeline, beginning with the characterization of vibration signals and culminating in the estimation of fatigue damage and remaining useful life. The paper proceeds as follows:

- First, the theoretical foundations are established by reviewing random processes, power spectral densities, and the use of frequency response functions to convert vibration excitation into local stress.
- Second, key fatigue concepts—spectral moments, S–N curves, and the Palmgren–Miner linear damage rule—are introduced to connect spectral descriptions to fatigue-life estimation.
- Third, the major frequency-domain methods for estimating stress-cycle amplitude distributions are presented, with particular emphasis on the Dirlik model, which remains the standard in engineering practice.
- Fourth, the full computational workflow is illustrated, showing how each component—measurement, signal processing, spectral characterization, material modeling, and damage accumulation—integrates into a coherent analysis framework.
- Finally, a review of applications of the previously introduced methods in various engineering domain will be proposed.

Although the exposition maintains mathematical rigor, the focus is placed on physical interpretation, engineering intuition, and practical implementation guidance. This foundational material sets the stage for subsequent comparative analyses involving time-domain and hybrid approaches as part of the broader PhD research.

2 Background

2.1 Fatigue Failure Under Random Vibration Loading

Engineering structures in real-world applications are frequently subjected to unpredictable, continuously fluctuating vibrational loads that pose a significant challenge to structural reliability and longevity [11]. As mentioned in Section 1, these random vibrational excitations do not follow deterministic or simple periodic patterns; instead, they are characterized by variable-amplitude loads that fluctuate in both global intensity and cyclic amplitude.

2.2 The Problem with Traditional Time-Domain Approaches

Traditionally, fatigue damage has been estimated using time-domain methods that analyze recorded stress or strain time-histories. These methods typically employ the rainflow counting algorithm [2] to extract individual stress cycles from the recorded signals, which are then accumulated using the Palmgren-Miner linear damage rule to calculate total damage. While this approach is conceptually straightforward and does not require simplifying assumptions about the loading process, it suffers from critical practical limitations.

First, accurate time-domain fatigue analysis requires very large time records—often spanning hours or days of simulated or measured data—to adequately capture the statistical characteristics of random processes. When stresses are obtained from finite element (FE) simulations, these time histories must be computed through time-step integration of the structural response. For complex structures, this implies solving the FE model at every time step, which becomes computationally expensive when long loading histories are required. For structures subjected to years of operational loading, generating, storing, and processing such extensive stress histories therefore becomes economically impractical. Second, the Rainflow counting process itself is computationally intensive, and when combined with Monte Carlo simulation techniques for generating time-domain stress signals from power spectral density (PSD) data, the total computational burden escalates dramatically [12].

2.3 Advantages of Frequency-Domain Spectral Methods

In contrast, frequency-domain spectral methods offer a fundamentally different and more efficient approach to fatigue estimation under random loading. Rather than working with time-domain stress histories, these methods operate directly on the power spectral density—a compact representation of how vibrational energy is distributed across frequencies [10]. This representation is particularly natural for structures subjected to random excitations, as random processes are naturally characterized by their spectral content rather than individual time samples.

Additionally, frequency-domain analysis circumvents the need for extensive time record generation and rainflow counting, instead employing analytical expressions—such as the Dirlik or Tovo-Benasciutti methods—that directly relate spectral moments to fatigue damage [7, 13]. Studies have reported computational speed improvements of 16 times or greater compared to equivalent time-domain approaches, without sacrificing accuracy for stationary, Gaussian random loading [14]. This efficiency gain becomes critical in design optimization scenarios where fatigue analysis must be performed at numerous structural locations across multiple design iterations.

2.4 Current State and Motivation for This Work

Despite these advantages, frequency-domain spectral methods remain less widely known and understood in engineering practice compared to traditional time-domain approaches. The mathematical foundations involve concepts from random vibration theory, spectral moments, and probabilistic cycle distribution models that can appear complex to practitioners unfamiliar with the field. Additionally, multiple spectral methods exist—Dirlik, Tovo-Benasciutti, Wirsching-Light, Zhao-Baker, and others—each with different assumptions, accuracy profiles, and ranges of applicability, making method selection non-obvious. Although, in 2004 Benasciutti [15] compared a group of frequency-domain methods, i.e., Wirsching–Light [16], Zhao–Baker [6], Dirlik [13], the empirical $\alpha 0.75$ [17], and Tovo–Benasciutti [18], and found that the Tovo–Benasciutti method matches the accuracy of the Dirlik method in terms of numerically simulated power spectral densities. A thorough study of fatigue evaluation for a multiaxial random loading was made by Lagoda et al. [19]. Experiment showed a good agreement with the fatigue-life estimate of the Wirsching–Light method. Throughout these studies, the results produced by the Dirlik method were again among the best and most consistent.

Hence, the motivation for this paper is to provide a clear, step-by-step pedagogical explanation of how frequency-domain methods transform raw vibration signals into fatigue and damage estimates in the case where we use the Dirlik method and the Palmgren-Miner linear damage accumulation rule. By following the logical progression from sensor measurements through signal processing, spectral analysis, material properties, and finally damage accumulation, readers will develop intuitive understanding of each stage and the mathematical principles underlying the approach. This foundational knowledge will establish a solid basis for comparing and integrating alternative analysis methods—time-domain and hybrid approaches—in subsequent work, and for

practitioners to confidently select and apply appropriate frequency-domain methods in design and reliability assessments.

3 Theoretical Background

To provide the necessary background for understanding frequency-domain fatigue methods and their associated definitions, an overview of the methods to extract the stress response from an acceleration signal is first introduced, then an introduction to stochastic process theory is proposed. Readers seeking a more comprehensive treatment and detailed derivations are referred to the foundational works of Shin and Hammond [20] and Newland [21].

3.1 Transitioning from vibration to stress

In fatigue analysis, the variable of interest is the stress time history $\sigma(t)$, since fatigue damage accumulates as a function of cyclic stress. However, what we often measure or simulate is a vibratory excitation such as base acceleration $a(t)$ or displacement $x(t)$. To analyze fatigue, it is therefore necessary to transform the measured vibration into the corresponding stress response at a given point in the structure. This transformation is achieved through the Frequency Response Function [22].

For a linear time-invariant system, the output $\sigma(t)$ (stress) is related to the input $a(t)$ (acceleration) through a convolution in the time domain:

$$\sigma(t) = h(t) * a(t) \tag{1}$$

where $h(t)$ is the impulse response function of the system. Taking the Fourier Transform [23] the convolution becomes a multiplication in the frequency domain:

$$\Sigma(f) = H(f)A(f) \tag{2}$$

where $\Sigma(f)$ is the Fourier transform of the stress signal $\sigma(t)$, $A(f)$ is the Fourier transform of the input acceleration $a(t)$, and $H(f)$ is the Frequency Response Function or transfer function describing the structure's dynamic sensitivity between input and output.

Establishing a mathematical model of the structure is the objective of modal analysis. The structural dynamics that can relate vibration to stress can be characterized during the design of the structure with the help of Finite Element Model (FEM) [24]. The linear structural dynamics is described in the frequency domain, which is why the frequency-domain methods for fatigue analysis are of great interest.

Complex structures can be viewed as linear, multi degree-of-freedom systems that are described by a system of second-order differential equations [25]:

$$[M]\{\ddot{X}\} + [C]\{\dot{X}\} + [K]\{X\} = \{f\} \tag{3}$$

where$[M]$ is the mass matrix, $[C]$ is the damping matrix,$[K]$ is the stiffness matrix, $\{X\}$ is the vector of degrees of freedom and $\{f\}$ is the excitation force vector. Furthermore, through modal analysis, the transfer function $H(f)$ from one point on the structure to the other can be deduced numerically, analytically or by experiment.

For a selected geometrical location on the structure the stress response spectra Σ (resp. σ) can be obtained by knowing the frequency response function as defined by equation 2 in the frequency domain (resp. by equation 1 in the time domain).

As specified earlier, the determination of this frequency response function can be numerical, analytical or experimental.

3.1.1 Numerical estimation of the FRF

In practical structural dynamics, the frequency response function (FRF) between an excitation point and a response point is often estimated numerically. This is typically done using a finite-element model or a

modal model of the structure once the dynamic characteristics—natural frequencies, damping ratios, and mode shapes—have been obtained. For linear systems, the FRF can be expressed using modal superposition, in which each vibration mode contributes independently to the overall response. A commonly used formulation represents the FRF $H(f)$ as the sum of the modal contributions [26]:

$$H(f) = \sum_{r=1}^{n} \frac{\phi_r(x)\,\phi_r(f)}{m_r(\omega_r^2 - \omega^2 + i2\zeta_r\omega_r\omega)} \tag{4}$$

where $\phi_r(x)$ and $\phi_r(f)$ are the modal participation factors at the response (stress) and excitation points, respectively. m_r, ω_r and ζ_r are the modal mass, natural frequency and damping ratio for mode r. And $\omega = 2\pi f$ is the forcing frequency.

This modal superposition formulation allows the prediction of the stress response at any structural location, even in the absence of direct measurements, provided that the modal model is properly validated. Modal decomposition techniques described by [12] and [27] demonstrate how this method forms the basis for estimating stress PSDs across complex structures. Although it provides a strong estimation of the structural dynamics, this approach requires a validated FE model and it often needs to be updated.

3.1.2 Analytical estimation of the FRF

In cases where the system behaves approximately as a single-degree-of-freedom (SDOF) or when an analytical model suffices, the FRF can be derived directly from classical vibration theory. For an SDOF system subjected to a base acceleration input, the FRF takes the form [28]:

$$H(f) = \frac{j(2\pi f)^2}{\omega_n^2 - (2\pi f)^2 + j\,2\zeta\,\omega_n(2\pi f)} \tag{5}$$

where ω_n is the natural frequency, ζ is the damping ratio, and j is the imaginary unit used to express the complex nature of the FRF. This analytical form provides intuitive insight into the system's dynamic amplification near resonance and can be extended to approximate multi-modal systems by superposing several SDOF contributions.

Although simplified, analytical FRFs are widely used for preliminary studies, design screening, or in scenarios where modal or experimental data are unavailable. In fact, their limited accuracy for complex geometries does not make them reliable for multi-modal spectra or mode coupling.

3.1.3 Experimental estimation of the FRF

The experimental approach is based on *modal testing*, where the system is excited using an impact hammer or shaker, and both the input (e.g., acceleration or force) and output (e.g., strain or stress) responses are measured. The FRF is then determined using spectral estimation techniques as described by [29]:

$$H(f) = \frac{S_{\sigma a}(f)}{S_{aa}(f)} \tag{6}$$

where $S_{\sigma a}(f)$ is the cross-spectral density between stress and acceleration, and $S_{aa}(f)$ is the input auto-spectrum [30]. A description of the power spectral density is given in Section 3.2.

This method inherently captures real boundary conditions, damping effects, and structural nonlinearities. It is the most direct approach to obtaining the dynamic sensitivity between an input excitation and local stress. Commonly used measurement methods include impact testing and shaker testing, with coherence analysis to assess signal reliability [28, 29]. However, this method requires measurement equipment and rigorous measurement practices.

3.2 Gaussian random processes

A stochastic process $X(t)$ is said to be a *Gaussian process* if, for every integer $n \geq 1$ and every finite set of time instants $t_1, t_2, \ldots, t_n$, the random vector

$$\mathbf{X} = [X(t_1), X(t_2), \ldots, X(t_n)]^\top$$

follows a multivariate normal distribution. Formally,

$$\mathbf{X} \sim \mathcal{N}(\boldsymbol{\mu}, \boldsymbol{\Sigma}),$$

where the mean vector $\boldsymbol{\mu} = [\mu(t_1), \ldots, \mu(t_n)]^\top$ and the covariance matrix $\boldsymbol{\Sigma}$ are defined as

$$\mu(t_i) = \mathbb{E}[X(t_i)], \qquad \Sigma_{ij} = \mathrm{Cov}(X(t_i), X(t_j)) = \mathbb{E}[(X(t_i) - \mu(t_i))(X(t_j) - \mu(t_j))].$$

A Gaussian process [31] is therefore fully characterized by its mean function $\mu(t)$ and autocovariance function $C_{XX}(t_1, t_2)$, and can be denoted compactly as

$$X(t) \sim \mathcal{GP}\big(\mu(t), C_{XX}(t_1, t_2)\big).$$

If the process is *stationary*, the mean is constant ($\mu(t) = \mu$) and the autocovariance depends only on the time lag $\tau = t_2 - t_1$, i.e. $C_{XX}(t_1, t_2) = C_{XX}(\tau)$. In that case, the *power spectral density* (PSD) [10] $S_{XX}(f)$ is defined as the Fourier transform of the autocovariance function:

$$S_{XX}(f) = \int_{-\infty}^{\infty} C_{XX}(\tau)\, e^{-j2\pi f \tau}\, d\tau.$$

In the context of vibration analysis, assuming a zero-mean stationary Gaussian process implies that the response amplitude is normally distributed and that the process is completely described by its second-order statistics ($\mu(t)$ and $C_{XX}(t_1, t_2)$). It is customary to use a one-sided power spectral density $G_{XX}(f)$, defined on the positive half-axis only. The statistical properties of a stationary process can be described by the moments of the power spectral density [32]. The general form for the ith spectral moment m_i is given by:

$$m_i = \int_0^{\infty} f^i G_{XX}(f) df \tag{7}$$

For a fatigue analysis, we will consider the power spectral density $S_{\sigma\sigma}(f)$ of our stress signal $\sigma(t)$ obtained via the frequency response function described in section 3.1. The moments we extract from the stress PSD describe how our stress response behaves. In subsequent analysis, only moments up to m_4 will be used.

The zeroth moment m_0 relates to the variance of the signal, the first moment m_1 relates to the mean frequency, the second moment m_2 relates to the bandwidth of the signal, and the fourth moment m_4 relates to higher order characteristics. From these moments, key parameters can be extracted to describe the behaviour of our stress signal:

- $v_0 = \sqrt{\frac{m_2}{m_0}}$, the expected positive zero-crossing rate which measures how "shaky" the signal is or how fast it oscillates. Intuitively if the spectrum is dominated by higher frequencies, the process crosses zero more often.
- $v_p = \sqrt{\frac{m_4}{m_2}}$, the expected peak occurrence frequency which measures the "choppiness" of the signal, or how many peaks occur between each zero-crossings. Intuitively, in a broad-spectrum noise-like signal, there can be many small peaks between crossings, giving a much higher v_p than v_0. In contrast for a smooth narrow-band wave $v_p \approx v_0$.
- $\alpha_i = \frac{m_i}{\sqrt{m_0 m_{2 \cdot i}}}$, the spread of the process, or the spectral width. Depending on the value of i this metric can have different interpretations.

The most commonly used value of i is 2 giving α_2 which is the negative of the correlation between the process

$X(t)$ and its second derivative $\ddot{X}(t)$ as described by Tovo [7]. It is also called the irregularity factor. It takes values from 0 to 1, the higher the value, the narrower the process in the frequency domain (single dominant frequency) and vice versa (multiple existing frequencies). Another parameter describing the bandwidth of the signal is Vanmarcke's parameters [32]:

$$\delta = \sqrt{1 - \alpha_1^2} \tag{8}$$

The difference between α_2 and Vanmarcke's parameter δ is that α_2 will describe how narrowly concentrated the PSD is (correlation between signal and curvature), and δ is a derived indicator that expresses the broadband nature of the process. Thus, for narrowband processes $\alpha_2 \to 1, \delta \to 0$, and for broadband processes $\alpha_2 \to 0, \delta \to 1$. Each of these parameters plays a crucial role in determining the intensity of fatigue life consumption. Their analytical derivation was rigorously established by Newland [21]. Figure 1 illustrates the visual difference between a broadband and a narrowband process. In the broadband process, we can see no apparent pattern and strong variation, illustrating the presence of multiple frequencies. In the narrowband process, the sinusoidal look of the signal illustrates the presence of a smaller number of frequencies.

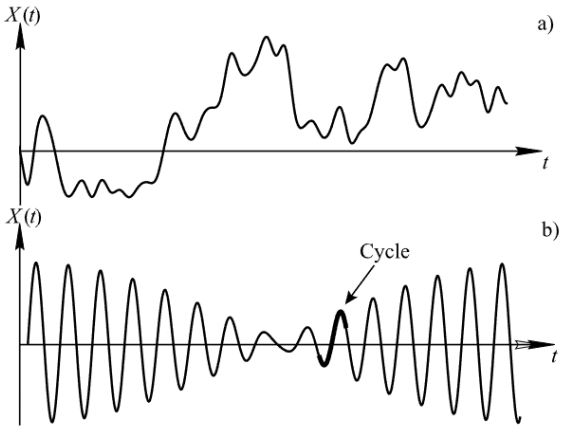

Figure 1: Example of wideband process (a) and narrowband process (b) (see Muniz et al. [33])

3.3 S-N Curves

The S-N curve (also called a Whöler curve or stress-life curve) is a fundamental tool in fatigue analysis that describes the relationship between the cyclic stress amplitude (S) applied to a material and the number of cycles until failure occurs [34]. Named after the pioneering work of August Whöler in the 19th century, S-N curves characterize the fatigue strength of materials and form the basis for predicting structural durability under cyclic loading. In the context of frequency-domain fatigue analysis, S-N curves are essential components that link the statistical properties of random stress to material failure predictions [35].

Some literature dealing with S-N curve models has been available since Weibull [36] discussed S-N curve models. Schutz [37] discussed the Basquin model [38] within the context of fatigue history for a period of 1838–1996. Kohout and Vechet [39] reviewed a few S-N curve models in relation to a newly proposed model. Some S-N curve models were overviewed by Nijssen [40]. Recently, Xiong and Shenoi [41] listed four S-N curve models including Basquin model as the generally accepted ones in a monograph. Buhran [42] proposed the latest review of S-N curves for composite materials giving a critical review of the models cited above. The proposed models in the cited literature can be classified into two groups depending on the approach considered (see Table 1 for consulting the formulas of each model):

- Deterministic models, such as the linear (see Basquin [38]), bilinear (Palmgren [3], Stromeyer [43], Speindel and Haibach [44]) and trilinear rules of sigmoidal curves (Stussi [45], Weibull [36], Kohout and Vechet [39]), among others.
- Probabilistic models, such as Bastenaire [46], Castillo and Canteli [47], Bolotin [48] and Pascual and Meeker [49], among others

Table 1: Proposed deterministic and probabilistic models in literature for the S–N curves (see Castillo and Fernández-Canteli [47]).

Model	**Expression**
Basquin [38]	$\log N = A - B\log S$
Stromeyer [43]	$\log N = A - B\log(S - S_0)$
Palmgren [3]	$\log(N + D) = A - B\log(S - S_0)$
Weibull [36]	$\log(N + D) = A - B\log\left(\frac{S-S_0}{S_{st}-S_0}\right)$
Stüssi [45]	$\log N = A - B\log\left(\frac{(S-S_0)}{(S_{st}-S)}\right)$
Bastenaires [46]	$\big(\log N - B\big)(S - S_0) = A\exp[-C(S - S_0)]$
Spindel–Haibach [44]	$\log(N/N_0) = A\log(S/S_0) - B\log(S/S_0) + B\left\{(1/\alpha)\log\big[1 + (S/S_0)^{-2\alpha}\big]\right\}$
Castillo–Canteli [47]	$\log(N/N_0) = \dfrac{\lambda + \delta\big(-\log(1-p)\big)^{\beta}}{\log(S/S_0)}$
Kohout–Vechet [39]	$\log\left(\frac{S}{S_\infty}\right) = \log\left(\frac{N+N_1}{N+N_2}\right)^b$
Pascual–Meeker [49]	$\log N = A - B\log(S - S_0)$

For practical reasons and as commonly adopted by the literature for frequency-domain analysis, we will go over the Basquin model as a reference.

Basquin's law, named after American metallurgist O. H. Basquin who introduced it in 1910, expresses the relationship between stress amplitude S and cycles to failure N_f as a power law [38]:

$$N_f = \frac{A}{S^b} \tag{9}$$

or equivalently in log-log form:

$$\log N_f = \log A - b\log S \tag{10}$$

where N_f is the number of cycles to failure, S is the stress amplitude or stress range (typically in MPa or Pa), A is the fatigue strength coefficient (material constant representing stress amplitude as N=1 cycle), and b (or B in Table 1) is the fatigue strength exponent (typically ranging from 3 to 13, depending on material), representing the slope of the S-N curve on log-log scale.

Values of the b coefficient allow us to interpret the behaviour of the material under stress cycles. The negative slope on the log-log plot means that higher stress amplitudes lead to shorter fatigue life. The steeper the slope (larger b value), the more sensitive the material is to stress changes. Materials with steep S-N curves show rapid life reduction with small stress increases, while materials with shallow sloped show more gradual life reduction.

For metals and alloys, the Basquin coefficients A and b depend on material properties and can be estimated or determined from limited data. For many steels, empirical correlations relate A to ultimate tensile strength u_t:

$$A \approx 0.9u_t \text{ for N= 1 cycle} \tag{11}$$

In some cases, this coefficient is rounded to $A = 1$. More refined correlations account for yield strength, hardness, and surface finish [50].

3.4 Palmgren-Miner Linear Damage Rule

The life expectancies of parts subjected to spectrum loading are commonly estimated from the empirical Palmgren-Miner damage law, introduced first by Palmgren [3] in the analysis of ball bearings and adapted by Miner [4] for aircraft structures.

Let n_i denote the number of stress cycles with a constant stress amplitude S_i and N_f is the number of cycles with the same amplitude to a specified extent of the damage ξ after which the component is considered to have failed. Miner [4] suggested that in a fatigue test at a constant stress amplitude S_i damage could be regarded to accumulate linearly with the number of cycles. Accordingly, if at a stress amplitude S_1 the component has a life of N_{1f} cycles, which corresponds to the amount of damage ξ, after n_1 cycles at the same stress amplitude, the amount of damage will be $\frac{n_1}{N_{1f}}\xi$. After n_2 stress cycles at the same stress amplitude S_2, characterized by a fatigue life of N_{2f} cycles, the amount of damage will be $\frac{n_2}{N_{2f}}\xi$ etc. [51]. Failure occurs when, at a certain stress amplitude S_m, the sum of the partial amounts of damage attains the amount ξ, i.e. when

$$\frac{n_1}{N_{1f}} + \frac{n_2}{N_{2f}} + \cdots + \frac{n_m}{N_{mf}} = 1 \tag{12}$$

is fulfilled. As a result, the analytical expression of the Palmgren-Miner rule becomes

$$\xi = \sum_{i=1}^{M} \frac{n_i}{N_{if}} \tag{13}$$

where N_{if} is the number of cycles to attain the specified amount of damage ξ at a constant stress amplitude S_i. Essentially, equation 13 is an additivity rule according to which the total number of stress cycles required to attain a specified level of damage ξ is obtained by adding the absolute durations n_i spent at each stress amplitude S_i, until the sum of the relative durations $\frac{n_i}{N_{if}}$ becomes unity. The fraction of expended fatigue life at a particular stress amplitude is the ratio of the number of stress cycles spent at this stress amplitude and the total number of stress cycles of the same stress amplitude needed to attain the specified level of damage (from zero initial damage). It is also assumed that the sequence in which the various stress amplitudes are imposed does not affect the fatigue life [51]. Subsequently we will refer to the accumulated damage as D. Practically, if D exceeds or is equal to unity, the material has entered a state of failure. Conversely, any value below unity will represent the amount of life (as a percentage) consumed by the cycles.

The definition given in equation 13 is set for a discrete number of cycles, commonly extracted from the rainflow counting algorithm [2] and a discrete number of stress amplitudes. In the case of frequency-domain methods, it it important to consider the accumulated damage over a continuous space of stress amplitudes where stress amplitudes follow a continuous probability distribution.

$$D = \int_0^\infty \frac{n(S)}{N_f(S)} dS = v_p.T \int_0^\infty \frac{p(S)}{N_f(S)} dS \tag{14}$$

or equivalently, the damage rate per unit time is:

$$\dot{D} = v_p \int_0^\infty \frac{p(S)}{N_f(S)} dS \tag{15}$$

where $p(S)$ is a probability density function of stress ranges or amplitudes, $N_f(S)$ is the number of cycles to failure at stress range S that is derived from the S-N curve in Section 3.3. The parameter v_p is the expected peak rate defined in Section 3.2. The reader will understand that statistical assumptions about the stress are paramount to use the continuous form of the Palmgren-Miner rule, as v_0 is built from the spectral moments of the stress PSD assumed as a stationary, random Gaussian process as mentioned in Section 3.2. The parameter T is the duration of the loading sample in seconds, and dS is the infinitesimal stress increment.

The transition from discrete to continuous is achieved by recognizing that in the discrete case n_i cycles occur at stress level S_i, whereas in the continuous case, the number of cycles in a stress range interval $[S, S + dS]$ is

$n(S)dS = v_p T p(s)dS$. This connection is fundamental to frequency-domain fatigue analysis where the Dirlik [13] or other spectral methods [6–8] provide the probability density function $p(S)$, enabling the calculation of damage without explicit time domain cycle counting.

Despite its widespread use and simplicity, extensive experimental testing has revealed several significant deficiencies of the Palmgren-Miner rule:

- Experimental data shows that the order of loading matters, contrary to the rule's assumptions. Specifically, the High-Low loading and the Low-High loading phenomena. For the first one, when high-stress cycles are applied first, following by low-stress cycles, the rule is non-conservative (predicts failure too late) [52]. Conversely, when low-stress cycles precede high-stress cycles the rule is conservative (predicts failure too early).
- High-stress overloads in a loading sequence can cause crack retardation due to residual stress effects (stress redistribution near the crack tip), actually reducing damage accumulation. Conversely, underloads can accelerate crack growth. The Palmgren-Miner rule cannot capture these nonlinear interactions [53, 54].
- For materials with a fatigue limit (e.g., steels), cycles below the endurance limit should theoretically cause no damage. However, some experimental evidence suggests that such subcritical cycles may have cumulative harmful effects when combined with higher-stress cycles. The Palmgren-Miner rule treats these as harmless (contributing zero damage), potentially missing subtle effects [53].

To address limitations of the linear Palmgren-Miner rule, researchers have developed nonlinear damage accumulation models that account for load interaction effects and sequence dependence.

One of the most popular alternatives is the Manson-Halford model [55], based on the concept of a nonlinear "damage curve" that shows how damage accumulates nonlinearly with cycle ratio:

$$D(A) = \sum_i (\frac{n_i}{N_i})^{q_i}, q_i = BN_i^{\mu} \tag{16}$$

where q_i is a material-dependent exponent that captures nonlinearity, and B, μ are material parameters. This model recognizes that damage accumulation is not linear but follows and accelerating curve, with damage increasing faster as the component approaches failure.

Other recent approaches based on continuum damage mechanics explicitly model the progressive degradation of material properties with cumulative cycles, leading to accelerated damage rates as failure approaches [56]. However, in the literature, and in the industry, the Palmgren-Miner rule is the most adopted method as it provides a simple, but not simpler way to model damage accumulation through the fatigue of a material under stress cycles.

4 Frequency-Domain Methods for Estimating Stress Range Probability Distributions.

The central challenge in frequency-domain fatigue analysis is to determine the probability function $p(S)$ of stress ranges, defined in Section 3.4, directly from the power spectral density without generating time-domain signals or applying rainflow counting. Due to the inherent complexity of pairing procedure peak-to-valley in the rainflow counting algorithm for a wideband process there is no explicit analytical solution for the cycle distribution, and consequently neither for the expected accumulated damage. For this reason researchers have developed numerous spectral methods that attempt to approximate the rainflow-counted stress range distribution using only spectral moments and bandwidth parameters derived from the PSD [57]. These methods vary in complexity, accuracy, and computational efficiency, and their performance depends strongly on the spectral characteristics of the loading (if the signal is narrowband or wideband) [12, 58]. In this section, we present how the idea of estimating stress range distribution was theorised by Rice [59], then we present the narrow-band (NB) approximation [60, 61] that is only appropriate for narrowband signals. The other methods are approriate for both narrow and wideband signal. In particular, the Wirsching-Light method (WL) [16], the $\alpha_{0.75}$ method (AL) [15], the

Jiao-Moan (JM) [62], the Gao-Moan method (GM) [14], the Zhao-Baker (ZB1, and ZB2) method [6], the Tovo-Benasciutti method (TB) [18], the Petrucci-Zucarello (PZ) [8], and finally, the Dirlik method (DK) [13]. Note that the $\alpha_{0.75}$ and the Wirshing-Light methods differ from the others in the way that they provide a correction factor to correct the narrow-band approximation for wideband processes.

4.1 Rice's method

In this framework of estimating the fatigue from the stress PSD, the key challenge lies in understanding the function of the rainflow cycle-counting algorithm in the time domain. Namely, its ability to construct a statistical distribution of stress ranges corresponding to individual cycles. The theoretical basis for developing a frequency-domain approximation of such a cycle distribution was introduced by Rice in 1944 [59], who derived an analytical expression for the probability density function of peak amplitudes, $p_p(a)$ directly from the power spectral density (PSD) of the process. In other words, his result tells us "*Given the PSD of a random vibration signal, what is the probability that its peaks will have a given amplitude a*". The equation of this distribution is given by:

$$p_p(a) = \frac{\sqrt{1-\alpha_2^2}}{\sqrt{2\pi}\sqrt{m_0}} e^{-\frac{a^2}{2m_0(1-\alpha_2^2)}} + \frac{\alpha_2 a}{m_0} e^{-\frac{a^2}{2m_0}} \Phi\left(\frac{\alpha_2 a}{\sqrt{m_0}\sqrt{1-\alpha_2^2}}\right) \tag{17}$$

where a is the peak amplitude, α_2 the irregularity factor, m_0 the zeroth statistical moment of the PSD. Both of these parameters are defined in Section 3.2. The parameter θ is the standard normal cumulative distribution function:

$$\Phi(z) = \frac{1}{\sqrt{2\pi}} \int_{-\infty}^{z} e^{-\frac{t^2}{2}} dt \tag{18}$$

Rice's formulation provides the probability distribution of peak amplitudes in a Gaussian random vibration directly from its power spectral density (PSD). It describes how likely different vibration peaks are to occur, linking the shape of the spectrum (through the bandwidth parameter α_2) to the irregularity of the time-domain signal. For a narrowband vibration (dominated by a single resonance), the peaks follow a Rayleigh-like distribution:

$$p_p(a) = \frac{a}{\sigma_X^2} e^{-\frac{a^2}{2\sigma_X^2}} \tag{19}$$

That is, a bell-shaped curve that starts at zero, peaks once, and then decays exponentially. While for a broadband excitation (energy spread over many frequencies), they approach a normal distribution [59].

4.2 Narrowband approximation

The narrowband approximation represents one of the foundational and simplest frequency-domain method, originally formulated by Miles [61] in 1956 and later refined by Bendat [60] in 1964. This method applies when the stress response is dominated by a single resonant frequency, producing a nearly sinusoidal time history with slowly varying amplitude—a condition characterized by the irregularity factor α_2 approaching unity. In fact, for a narrowband process it is reasonable to assume that every peak coincides with a cycle and that consequently, the cycle amplitudes are Rayleigh distributed. That is, the stress range amplitudes follow a Rayleigh probability distribution. Intuitively, it is where the signal behaves like a nearly sinusoidal process with random phase. In such cases, most stress cycles have moderate amplitudes, while very large cycles are rare, following the Rayleigh law [63].

The probability density function of stress ranges S is:

$$p_{NB}(S) = \frac{S}{m_0} \exp\left(-\frac{S^2}{m_0}\right) \tag{20}$$

where m_0 is the zeroth spectral moment defined in Equation 7. The corresponding fatigue damage rate per unit time is:

$$\dot{D_{NB}} = v_p \int_0^\infty p_{NB}(S).\frac{S^b}{A}dS = v_p \frac{(\sqrt{2m_0})^b}{A}\Gamma(1+\frac{b}{2}) \tag{21}$$

where $\Gamma(.)$ is the gamma function. That is, a generalization of the factorial function to non-integer numbers. The parameter v_p is the expected peak rate, and A, b are the S-N curve parameter as defined in Section 3.3.

Equation 20 illustrates how empirical and how specific to narrowband signals the method is. In fact, the narrowband approximation is highly conservative (overestimates damage) for wideband loading, where many small intermediate cycles occur between major peaks. For typical engineering structures with Vanmarcke [32] bandwidth parameter $\delta = 0.1$ to 0.95 defined using Equation 8, errors can exceed 100% or more. As the spectrum becomes broader, the narrowband assumption breaks down completely, making correction or alternative methods necessary.

4.3 Wirsching-Light correction method

Recognizing the limitations of the narrowband approximation for wideband loading, Wirsching and Light (1980) [16] proposed an empirical correction factor that adjusts the narrowband damage estimate based on the spectral bandwidth parameter α_2. Wideband processes contain many small cycles that contribute less to fatigue damage than the large cycles captured by the narrowband approximation. The correction factor reduces the overestimated narrowband damage to better match rainflow-counted results [64].

The method is defined as follows:

$$D_{WL} = \rho_{WL}.D_{NB} \tag{22}$$

where D_{NB} is the narrow band approximation obtained with Equation 21, and ρ_{WL} is defined as:

$$\rho_{WL} = a(b) + [1 + a(b)](1-\epsilon)^{c(b)} \tag{23}$$

with the spectral width parameter $\epsilon = \sqrt{1-\alpha_2^2}$ and the best fitting parameters $a(.)$ and $c(.)$ dependent on the S-N slope b as defined in Section 3.3:

$$a(b) = 0.926 - 0.033b \ , \ c(b) = 1.578b - 2.323 \tag{24}$$

where authors used the S-N slope b values of 3, 4, 5 and 6 for the simulations. They observed that the correction factor $\rho_{WL} < 1$ decreases as α_2 decreases (spectrum widens), reducing the damage estimate. The Wirsching-Light method improves upon the narrowband approximation but tends to remain somewhat conservative, particularly for very wideband spectra. Its accuracy depends on the S-N curve slope b and it has been largely superseded by more sophisticated methods [63].

4.4 Alpha 0.75 correction method

The alpha 0.75 method, developed by Benasciutti and Tovo [15], introduces a new bandwidth parameter specifically tuned through extensive Monte Carlo simulations to provide better correction for wideband processes. The corrected damage rate is defined as follows:

$$D_{\alpha_{0.75}} = \alpha_{0.75}^2.D_{NB} \tag{25}$$

where the bandwidth parameter $\alpha_{0.75} = \frac{m_{0.75}}{\sqrt{m_0 m_{1.5}}}$ with fractional-order spectral moments $m_{0.75}$ and $m_{1.5}$ computed from the PSD. The fractional-order moments capture intermediate spectral characteristics that better describe the distribution of stress cycles in wideband processes. The $\alpha_{0.75}$ parameter provides a more sensitive measure of spectral bandwidth than α_2 [15]. A common conclusion in the literature is that the alpha 0.75 method

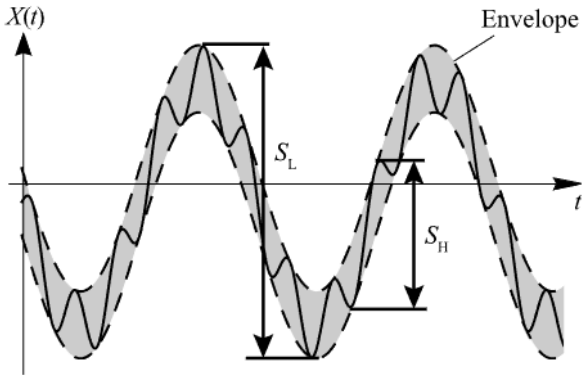

Figure 2: Schematic illustration of a bimodal process identifying both low and high frequency components.

generally overestimates damage but with smaller errors (typically within 4%) compared to Wirsching-Light. It has shown good accuracy for a wide range of spectral shapes [63].

4.5 Jiao-Moan method

The Jiao-Moan method [62] is one of the first proposals dealing with bimodal processes, that is, a power spectral density with two well-separated modes. It is known for being an accurate prediction method for bimodal vibrations fatigue included in international offshore engineering code (see ISO 19901-7). Methods by Sakai-Okamura [65] and Fu and Cebon [66] were also successfully applied [33].

The original proposal by Jiao and Moan assumes any random process $X(t)$ can be expressed as a sum of two independent narrowband processes, that is,

$$X(t) = X_H(t) + X_L(t) \tag{26}$$

where X_H and X_L represent the high and low frequency components in which the bimodal signal can be decomposed. Figure 2 presents and illustrative example of a bimodal signal, from which the rainflow cycle fatigue method could extract two type of cycles: large cycles with amplitude S_L, and small cycles with amplitude S_H. As a result, the amplitude stress distribution is derived as a combination of two narrowband process by means of the convolution integral, leading to:

$$p_{JM}(S) = \sqrt{\frac{\lambda_1^*}{2\pi}}\,\exp(-\frac{S^2}{2\lambda_1^*}) + \sqrt{\lambda_2^*}S\,\exp(-\frac{S^2}{2})\Phi(\sqrt{\frac{\lambda_2^*}{\lambda_1^*}}S) \tag{27}$$

where λ_1^* and λ_2^* are the bandwidth parameters of each narrowband process (α_2 described in Section 3.2).

4.6 Gao-Moan method

The Gao-Moan method developed in 2007 [14] is an analytical approach specifically designed for trimodal (three peaks) spectra, naturally developed after the Jiao-Moan approach.

The method decomposes a complex multimodal spectrum into contributions from individual spectral peaks, treating each as an independent narrowband process. The total damage is then computed as a weighted combination of damages from each mode, accounting for their statistical interaction. The fatigue-damage intensity D_{GM} is the sum of the high-frequency process $R_H(t)$, the intermediate-frequency process $R_M(t)$ and the low-frequency process $R_L(t)$ contributions, each being narrow-banded and having a Rayleigh-distributed amplitude with the respective variances equal to $\sigma_H, \sigma_M, \sigma_L$:

$$D_{GM} = D_P + D_Q + D_H \tag{28}$$

where D_P and D_Q are damage intensities due to the processes $R_P(t)$ and $R_Q(t)$, respectively:

$$R_P(t) = R_H(t) + R_M(t)\ ,\ R_Q(t) = R_H(t) + R_M(t) + R_L(t) \tag{29}$$

The damage component D_H is determined using equation 21. Equation 15 is used for D_P and D_Q with the probability function $p(S)$ being a Rayleigh distribution, and where the expected zero-crossing rate v_0 is used instead of the expected peak rate v_p, and is calculated with:

$$v_{0P} = \sqrt{m_{2H}\delta_H^2}\frac{\sigma_M}{(\sigma_H^2 + \sigma_M^2)} \tag{30}$$

$$v_{0Q} = \sqrt{m_{2H}\delta_H^2 + m_{2M}\delta_M^2 + m_{2L}} \times [\frac{2\sigma_L\sqrt{\sigma_H^2 + \sigma_M^2 + \sigma_L^2} - \pi\sigma_H\sigma_M}{2(\sqrt{\sigma_H^2 + \sigma_M^2 + \sigma_L^2})^3} + \frac{2\sigma_H\sigma_M \arctan\frac{\sigma_H\sigma_M}{\sigma_L\sqrt{\sigma_H^2+\sigma_M^2+\sigma_L^2}}}{2(\sqrt{\sigma_H^2 + \sigma_M^2 + \sigma_L^2})^3}] \tag{31}$$

where δ_H and δ_M are Vanmarcke's parameters from Equation 8, calculated for the processes $R_H(t)$ and $R_M(t)$, respectively. The probability density functions for the sum of two or more random variables (also needed for calculating Equation 15) are determined by means of the convolution integral:

$$p_{a,HM} = \int_0^\infty p_{a,H}(S)p_{a,M}(t-S)dS \tag{32}$$

$$p_{a,HML} = \int_0^\infty p_{a,HM}(S)p_{a,L}(t-S)dS \tag{33}$$

where $p_{a,HM}$ and $p_{a,HML}$ are the cycle-amplitude probability densities of the respective narrow-band processes. Hermite integration was used by Gao and Moan to calculate the distribution of the sum of the multiple Rayleigh random variables [12, 14].

While theoretically elegant, the Gao-Moan method requires evaluation of fractional-order integrals and has been found to have lower accuracy than empirical methods (Dirlik, Tovo-Benasciutti) for general wideband spectra, because it cannot fully capture the interaction between low-frequency and high-frequency modes.

4.7 Zhao-Baker method

The Zhao-Baker method (1992) [6] was among the first to approximate the rainflow-cycle amplitude distribution using a combination of theoretical assumptions and empirical fitting to Monte Carlo simulations. The method models the stress range distribution as a weighted combination of a Weibull distribution (capturing smaller cycles) and a Rayleigh distribution (representing larger cycles):

$$p_{ZB}(Z) = \underbrace{w\alpha\beta Z^{\beta-1}e^{-\alpha Z^\beta}}_{\text{Weibull}} + \underbrace{(1-w)Ze^{-Z^2/2}}_{\text{Rayleigh}} \tag{34}$$

where Z is the normalized amplitude defined as:

$$Z = \frac{S}{\sqrt{m_0}} \tag{35}$$

and w is the weighting factor defined by:

$$w = \frac{1-\alpha_2}{1 - \sqrt{\frac{2}{\pi}}\Gamma(1+\frac{1}{\beta})\alpha^{-1/\beta}} \tag{36}$$

and α and β are the Weibull parameters [12] determined from the spectral moments as defined in Equation 7:

$$\alpha = 8 - 7\alpha_2 \ , \ \beta = \begin{cases} 1.1, & \alpha_2 < 0.9 \\ 1.1 + 9(\alpha_2 - 0.9), & \alpha_2 \geq 0.9 \end{cases} \tag{37}$$

An improved version, the Zhao-Baker 2 (ZB2), modifies the calculation of the bandwidth parameter α by introducing:

$$\alpha = d^{-\beta} \tag{38}$$

where d is found as the root of a nonlinear equation involving gamma functions and spectral moments [17].

The literature [6, 12] agrees that the enhanced Zhao-Baker method (ZB2) has been found to provide excellent accuracy for automotive-type spectra with multiple modes and broad bandwidth. Comparative studies have shown it to be among the best-performing methods alongside Dirlik and Tovo-Benasciutti, and it is the only method providing consistently conservative (safe-side) estimates for typical automotive test profiles [17].

4.8 Tovo–Benasciutti method

The Tovo–Benasciutti (TB) [7, 15] method is one of the most widely used frequency-domain approaches for estimating fatigue damage under random vibration loading. It improves on traditional narrow-band approximations by providing an accurate estimate of the rainflow cycle distribution for wide-band processes, while remaining computationally efficient. The method relies solely on the spectral moments of the stress Power Spectral Density (PSD), making it suitable for use in conjunction with finite element analyses and random vibration test specifications [58].

Fatigue damage depends on the joint distribution of cycle amplitudes s and mean values m obtained by rainflow counting. For a general wide-band process, no exact analytical form of this distribution exists. The TB method postulates that the true rainflow distribution lies between two theoretical limit distributions:

- Level-Crossing Counting (LCC): cycles formed by pairing extrema with zero-mean crossings.
- Range Counting (RC): cycles formed by pairing each peak with the next valley.

These correspond to upper and lower bounds on the cycle amplitudes, respectively. The TB method approximates the rainflow amplitude–mean distribution as a weighted mixture of the two:

$$p_{\mathrm{TB}}(s, m) = w\, p_{\mathrm{LCC}}(s, m) + (1 - w)\, p_{\mathrm{RC}}(s, m), \tag{39}$$

where w is a bandwidth-dependent weight. Both p_{LCC} and p_{RC} depend solely on the PSD moments m_0, m_1, m_2, and m_4. The total fatigue damage is the weighted sum of damages from each limit distribution:

$$D_{\mathrm{TB}} = wD_{\mathrm{LCC}} + (1 - w)\, D_{\mathrm{RC}}. \tag{40}$$

The following approximations hold:

$$D_{\mathrm{LCC}} = D_{\mathrm{NB}} \tag{41}$$

$$D_{\mathrm{RC}} \approx \alpha_2^{b-1} D_{\mathrm{NB}} \tag{42}$$

where D_{NB} is the classical narrow-band damage (Miles/Bendat [60, 61] result described in Section 20), b is the inverse S–N slope, and α_2 is the irregularity factor.

Substituting gives the practical TB formula:

$$D_{\mathrm{TB}} \approx \left[w + (1-w)\,\alpha_2^{b-1}\right] D_{\mathrm{NB}} \tag{43}$$

4.8.1 Weight function

The most commonly used expression for the weight factor w is the refined form proposed in [18]:

$$w = \frac{(\alpha_1 - \alpha_2)\left[1.112\,(1 + \alpha_1\alpha_2 - \alpha_1 - \alpha_2)\,e^{2.11\alpha_2} + (\alpha_1 - \alpha_2)\right]}{(1-\alpha_2)^2} \tag{44}$$

where

$$\alpha_1 = \frac{m_1}{\sqrt{m_0 m_2}}, \qquad \alpha_2 = \frac{m_2}{\sqrt{m_0 m_4}}. \tag{45}$$

These parameters quantify the spectral bandwidth and the irregularity of the process.

An alternative expression based on fractional-order spectral moments was also proposed:

$$w_3 = \frac{\alpha_{0.75}^2 - \alpha_2^2}{1 - \alpha_2^2}, \qquad \alpha_{0.75} = \frac{m_{0.75}}{\sqrt{m_0 m_{1.5}}}, \tag{46}$$

which provides marginally improved accuracy in some cases, but is less widely adopted in practice.

The TB method has a clear physical meaning:

1. Cycle pairing behavior depends on bandwidth: Narrow-band signals exhibit nearly sinusoidal oscillation, with peaks and valleys occurring in regular alternation. This makes rainflow cycles nearly identical to LCC cycles ($w \to 1$).
2. Wide-band signals produce irregular clusters of peaks: In wide-band processes, peaks tend to occur in clusters and many small cycles appear. Rainflow cycles then resemble RC cycles ($w \to 0$).

Thus the TB method approximates how the physics of a random vibration process influences the distribution of damaging cycles [18].

4.9 Petrucci-Zucarello method

This method was proposed by Petrucci and Zuccarello (PZ) in 2004 [8] who sought a connection between the moments of the probability density of the equivalent Goodman stress and the parameters α_1, α_2, b, and γ, the last of these being the ratio:

$$\gamma = \frac{X_{max}}{S_u} \tag{47}$$

where X_{max} is the absolute maximum value of the stress process and S_{ut} is the material tensile strength. The PZ method implicitely predicts equivalent stress ranges by calculating the Goodman equivalent stress range [67]:

$$r_e = \frac{r}{1 - \frac{m}{S_u}} \tag{48}$$

where r is the original stress range, m is the range mean, and S_{ut} is the tensile strength. The expression for calculating the damage intensity is:

$$D_{PZ} = \frac{1}{A} v_p \sqrt{m_0^b}\, e^{\psi(\alpha_1, \alpha_2, k, \delta)} \tag{49}$$

where v_p is the expected peak rate and m_0 the zeroth spectral moment, defined in Section 3.2. The approximation function $\psi(.)$ [8] is given by:

$$\Psi(\alpha_1, \alpha_2, k, \gamma) = \frac{(\Psi_2 - \Psi_1)}{6}(b-3) + \Psi_1 + \left[\frac{2}{9}(\Psi_4 - \Psi_3 - \Psi_2 + \Psi_1)(k-3) + \frac{4}{3}(\Psi_3 - \Psi_1)\right](\gamma - 0.15) \quad (50)$$

where the coefficients Ψ_1 to Ψ_4 are given as polynomials:

$$\begin{aligned}
\Psi_1 &= -1.994 - 9.381\alpha_2 + 18.349\alpha_1 \\
&\quad + 15.261\alpha_1\alpha_2 - 1.483\alpha_2^2 - 15.402\alpha_1^2 \\
\Psi_2 &= 8.229 - 26.510\alpha_2 + 21.522\alpha_1 \\
&\quad + 27.748\alpha_1\alpha_2 + 4.338\alpha_2^2 - 20.026\alpha_1^2 \\
\Psi_3 &= -0.946 - 8.025\alpha_2 + 15.692\alpha_1 \\
&\quad + 11.867\alpha_1\alpha_2 + 0.382\alpha_2^2 - 13.198\alpha_1^2 \\
\Psi_4 &= 8.780 - 26.058\alpha_2 + 21.628\alpha_1 \\
&\quad + 26.487\alpha_1\alpha_2 + 5.379\alpha_2^2 - 19.967\alpha_1^2
\end{aligned}$$

with α_1 and α_2 taken from the definition given in Section 3.2. It shows the PZ method is a practical, easy-to-use option for quick fatigue estimates from vibration PSDs, especially when bandwidth is not extreme. However, for critical applications or highly complex frequency content, Dirlik's method remains preferred due to its superior accuracy and validation across a wide range of structural problems.

4.10 Dirlik method

The Dirlik method (1985) [13] is the most extensively validated and widely adopted frequency-domain method in both research and commercial software (nCode DesignLife, Ansys, Simulia Fe-safe, CAEfatigue). Developed by Turan Dirlik through extensive Monte Carlo simulations involving 70 different PSD patterns (rectangular bimodal and smooth spectra), it provides an empirical closed-form formula for the rainflow-cycle amplitude probability density.

Dirlik recognized that the rainflow-counted stress range distribution exhibits a characteristic multi-modal shape: a large number of small-amplitude cycles (captured by an exponential distribution) combined with medium and large-amplitude cycles (captured by two Rayleigh distributions with different scale parameters). The method combines these three component distributions in a weighted mixture, where the weights and parameters are determined purely from spectral moments m_0, m_1, m_2, m_4 [12].

The Dirlik probability density function for normalized stress ranges $Z = \frac{S}{2\sqrt{m_0}}$ is:

$$p_D(Z) = \frac{1}{2\sqrt{m_0}}\Big[\underbrace{\frac{D_1}{Q}e^{-Z/Q}}_{\text{Exponential term}} + \underbrace{\frac{D_2 Z}{R^2}e^{-Z^2/(2R^2)}}_{\text{Rayleigh (scale=R)}} + \underbrace{D_3 Z e^{-Z^2/2}}_{\text{Rayleigh (scale=1)}}\Big] \quad (51)$$

where the parameters D_1, D_2, D_3, Q, R and computed from the spectral moments as follows:

$$D_1 = \frac{2(x_m - \alpha_2^2)}{1 + \alpha_2^2} \quad (52)$$

$$R = \frac{\alpha_2 - x_m - D_1^2}{1 - \alpha_2 - D_1 + D_1^2} \quad (53)$$

$$D_2 = \frac{1 - \alpha_2 - D_1 + D_1^2}{1 - R} \quad (54)$$

$$D_3 = 1 - D_1 - D_2 \tag{55}$$

$$Q = \frac{1.25(\alpha_2 - D_3 - D_2 R)}{D_1} \tag{56}$$

with α_2 the spectral bandwidth parameter defined in Section 3.2.

Once $p_D(S)$ is obtained, we can calculate the damage rate:

$$\dot{D_D} = v_p \int_0^\infty p_D(S).(\frac{S}{A})^b dS \tag{57}$$

This integral is similar to the continuous Miner's rule form described in Equation 15.

However, the authors also proposed a closed form equation of the expected damage:

$$\dot{D_D} = \frac{1}{A} v_p m_0^{\frac{b}{2}} [D_1 Q^b \Gamma(1+b) + (\sqrt{2})^b \Gamma(1+\frac{b}{2})(D_2 |R|^b + D_3)] \tag{58}$$

Multiple comparative studies [12, 58, 68, 69] have confirmed Dirlik's method as one of the most accurate and reliable frequency domain methods thanks to its closed form formula, extensive validation, consistent accuracy and efficiency. Although, while Dirlik is highly accurate for stationary Gaussian processes, it shares the common limitation of all spectral methods: it assumes linearity, stationarity, and Gaussian distribution. For non-Gaussian loading, nonlinear systems, or transient excitations, modified approaches or time-domain methods may be necessary. Moreover, like any other methods in the frequency domain, it is based on the correct computation of spectral moments, and beyond that, the correct computation of the PSD (Section 3.2) and the Frequency Response Function (Section 3.1). Being built upon sensitive bricks allows for a possible error propagation.

Figure 3 illustrates the different methods of estimating the rainflow cycle distribution in a practical example on non Gaussian data provided by the Direction Générale de l'Armement. We can see that the Dirlik method is the best fit for the cycle-stress range distribution, and that Zhao-Baker is also a strong fit. In general it seems that the methods who are built upon a mixture of multiple laws (mainly exponential, Rayleigh, and Weibull) are the ones that capture most of the cycle distribution. The results we obtain are similar to those obtained by Nieslony et al. [70].

Table 2 summarizes the proposed stress amplitudes distribution in literature previously detailed. Only those authors that define explicitly distribution for the stress amplitudes are here included. Table 3 summarizes the proposed damage models of the frequency domain presented in the previous sections.

Table 2: Proposed rainflow cycle distributions in frequency domain methods.

Rainflow cycle distribution	**Expression**
Narrowband approximation [61]	$p_{NB}(S) = \frac{S}{\sqrt{m_0}^2} \exp(-\frac{S^2}{2\sqrt{m_0}^2})$
Dirlik method [13]	$p_D(Z) = \frac{1}{2\sqrt{m_0}}[\frac{D_1}{Q} \exp(\frac{-Z}{Q}) + \frac{D_2 Z}{R^2} \exp(\frac{-Z^2}{2R^2}) + D_3 Z \exp(\frac{-Z^2}{2})]$
Zhao-Baker method [6]	$p_{ZB}(Z) = w\alpha\beta Z^{\beta-1} \exp(-\alpha Z^\beta) + (1-w) Z \exp(\frac{-Z^2}{2})$
Tovo-Benasciutti method [7]	$p_{TB}(s,m) = w p_{LCC}(s,m) + (1-w) p_{RC}(s,m)$

5 Framework for Fatigue Life and Damage Estimation

Frequency-domain fatigue analysis provides a continuous and systematic method that connects vibration measurements, structural dynamics, and material fatigue properties into a single predictive process. Unlike time-domain approaches that rely on direct rainflow cycle counting, this method uses the statistical and spectral

Table 3: Proposed fatigue damage models in frequency domain methods.

Fatigue damage model	**Expression**
Narrowband approximation [61]	$\dot{D_{NB}} = v_p \frac{(\sqrt{2m_0})^b}{A} \Gamma(1+\frac{b}{2})$
Wirshing-Light method [16]	$\dot{D_{WL}} = a(b) + [1+a(b)](a-\epsilon)^{c(b)}.\dot{D_{NB}}$
$\alpha_{0.75}$ method [15]	$\dot{D_{\alpha}} = \alpha_{0.75}^2.\dot{D_{NB}}$
Jiao-Moan method [62]	$\dot{D_{JM}} = p_{JM}.\dot{D_{NB}}$
Gao-Moan method [14]	$\dot{D_{GM}} = \dot{D_P} + \dot{D_Q} + \dot{D_H}$
Dirlik method [13]	$\dot{D_D} = v_p \int_0^{\infty} p_D(S).(\frac{S}{A})^b dS$
Zhao-Baker method [6]	$\dot{D_{ZB}}(S) = \frac{v_0}{A}.\sqrt{m_0}^b [w.\alpha^{-b/\beta}\Gamma(1+\frac{b}{\beta}) + (1+w)2^{b/2}\Gamma(1+\frac{b}{2})]$
Tovo-Benasciutti method [7]	$\dot{D_{TB}} \approx [w+(1-w)\alpha_2^{b-1}]\dot{D_{NB}}$
Pettrucci-Zucarello method [8]	$\dot{D_{PZ}} = \frac{1}{A} v_p \sqrt{m_0^b} e^{\psi(\alpha_1,\alpha_2,k,\delta)}$

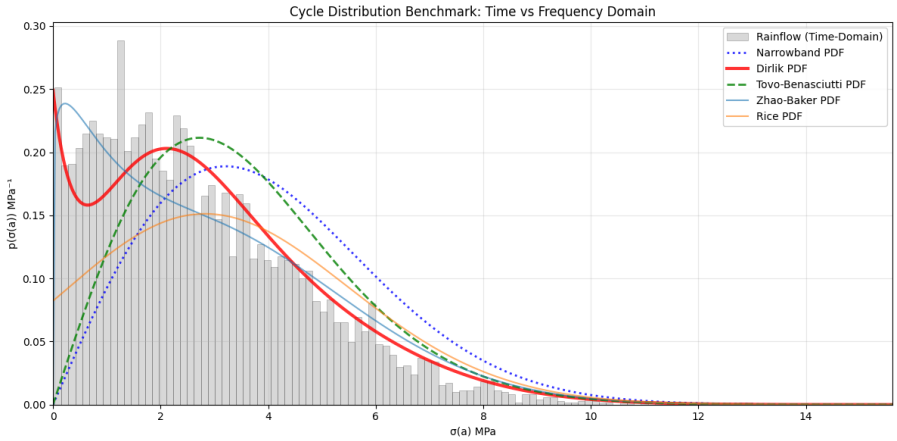

Figure 3: Different models proposed in the literature for the rainflow cycle distribution estimation. Built over SOPEMEA data provided by the Direction Générale de l'Armement. The data is non Gaussian and sampled over 2 seconds.

properties of the stress response to estimate fatigue damage analytically. The following paragraphs summarize the main stages of this process, linking each step to its physical meaning and key theoretical contributions. Table 4 summarizes the process sequentially, the physical meaning and key equations of each step.

5.1 Measurement and signal acquisition

The process begins with the measurement of vibratory excitation and response, typically through accelerometers or displacement sensors placed on the structure (Section 3.2). These signals represent how the structure reacts to its environment—road-induced vibration in vehicles, wind excitation in turbines, or launch loads in aerospace systems. The measured signal is usually expressed as acceleration or displacement as a function of time. At this stage, the objective is to obtain a representative record of the operational vibration environment that will later serve as input for fatigue analysis.

5.2 Transfer function and structural dynamics

Because fatigue damage depends on stress rather than vibration level, it is essential to transform the measured vibration into the corresponding local stress response. This transformation is defined by the Frequency Response Function (FRF), denoted $H(f)$, which represents how each frequency component of the input vibration contributes to the output stress at a specific location (Section 3.1). The FRF encapsulates the structure's stiffness, damping, and modal behavior.

There are three established ways to determine $H(f)$:

- Experimental modal analysis: measured directly through controlled vibration tests.
- Numerical model superposition: derived from FEM by summing modal contributions according to natural frequencies and damping.
- Simplified analytical model: used when the structure behaves approximately as a SDOF system.

In essence, this step builds the bridge between measured vibration and structural stress, establishing the physical pathway by which external excitations translate into material strain energy.

5.3 Stress spectral characterization

Once the FRF is defined, the stress power spectral density (PSD) can be calculated from the vibration PSD. The stress PSD describes how the stress energy is distributed across frequencies — highlighting which modes contribute most to fatigue. Whereas a Fourier transform provides instantaneous amplitude and phase, the PSD gives a statistical description of signal power versus frequency, making it ideal for the random, stationary vibration environments encountered in most practical cases (Section 3.2). At this stage, the structure's spectral response to dynamic loads becomes a compact representation of its fatigue-relevant behavior.

5.4 Spectral moments and statistical parameters

From the stress PSD, a set of spectral moments is computed — numerical integrals that characterize the shape and bandwidth of the spectrum. These moments, introduced by Vanmarcke (1972), allow one to extract key statistical measures such as the zero-crossing rate, peak rate, and irregularity factor. Physically, these parameters describe how "irregular" or "narrowband" the stress process is — that is, whether the vibration is dominated by a single resonance or spread over many frequencies (Section 7).

A high irregularity factor indicates a narrowband process where stress cycles resemble nearly sinusoidal oscillations, whereas a low value corresponds to broadband behavior with many overlapping frequencies. This distinction is crucial because the type of process determines which fatigue damage models are most appropriate.

5.5 Material properties and fatigue strength

The next step introduces the material's fatigue behavior via the S–N curve (or Wöhler curve), which expresses the relationship between stress range and fatigue life. Following Basquin's law (1910), this relationship is

represented by two constants — a fatigue strength coefficient and a fatigue exponent — that capture how quickly a material degrades with increasing stress amplitude (Section 3.3). These parameters can be obtained experimentally or from material databases. At this stage, the structural response (from Steps 1–4) is now linked to the material's intrinsic fatigue resistance.

5.6 Stress range distribution (Dirlik's model)

To estimate how often each stress amplitude occurs, the Dirlik method (Dirlik, 1985) is applied. It analytically derives the probability density function of stress ranges directly from the spectral moments of the stress PSD. Physically, Dirlik's model provides a statistical description of the stress cycle population — identifying how many cycles of a given amplitude the structure experiences under random vibration (Section 4.10).

The model represents this probability as a mixture of three distributions:

- an exponential term accounting for small stress cycles
- a Rayleigh term for medium cycles
- and another Rayleigh term scaled differently, for large cycles

This formulation efficiently reproduces the results of time-domain rainflow counting but without requiring explicit cycle extraction.

5.7 Damage accumulation (Palmgren-Miner integration)

Once the stress range distribution is known, fatigue damage accumulation can be estimated using the Palmgren–Miner linear damage rule. This rule states that each stress cycle consumes a fraction of the material's fatigue life, proportional to the ratio of experienced cycles to cycles to failure at that stress level. By integrating the Dirlik distribution with the S–N curve, one obtains the damage rate, or fatigue consumed per unit time (Section 3.4).

The total accumulated damage is then obtained by multiplying this rate by the operating duration. When the total reaches unity, fatigue failure is predicted. This continuous integration approach eliminates the need for discrete cycle counting and allows smooth combination of vibration statistics and material data.

5.8 Life estimation and decision criteria

From the total damage estimate, the remaining useful life can be computed by inverting the damage rate. If the accumulated damage over the mission duration is less than unity, the structure is considered safe; otherwise, fatigue failure is expected before the target time. This step connects the statistical results to practical engineering decisions, enabling fatigue-based life prediction, inspection scheduling, or design optimization.

5.9 Practical and computational advantages

Compared with time-domain fatigue analysis, this frequency-domain framework is significantly more efficient. Because it operates on PSDs rather than full time histories, it drastically reduces computation time and storage requirements while maintaining high accuracy for stationary, Gaussian processes. It also integrates naturally with finite element models, allowing engineers to evaluate fatigue life at multiple structural points in parallel.

5.10 Limitations and applicability

Despite its power, the frequency-domain approach assumes linearity, stationarity, and Gaussianity of the vibration process. It is therefore best suited for structures responding linearly to broadband, stationary excitation — such as vehicle chassis, aircraft panels, or electronic enclosures under random loads. For transient or nonlinear problems (e.g., impacts, shock, or frictional contacts), time-domain or hybrid methods remain necessary.

Table 4: Summary of stages from vibration measurement to fatigue life estimation.

Stage	Physical Meaning	Key Equation
Measurement	Raw vibration response	$a(t)$ or $x(t)$
Transfer Function	Vibration-to-stress relationship	$H(f) = \dfrac{\sigma(f)}{a(f)}$
Stress PSD	Stress energy distribution vs. frequency	$G_{\sigma\sigma}(f) = \lVert H(f) \rVert^2 G_{aa}(f)$
Spectral Moments	Statistical characterization	$m_i = \int_0^\infty f^i \, G_{\sigma\sigma}(f) \, df$
Dirlik Parameters	Stress distribution decomposition	D_1, D_2, D_3, Q, R from m_0, m_2, m_4
Stress Distribution	Probability of stress cycle amplitudes	$p_{\text{Dirlik}}(S)$ (3-component mixture)
S–N Curve	Material fatigue strength	$N_f(S) = (\dfrac{A}{S})^b$
Damage Rate	Fatigue consumption per second	$\dot{D} = \nu_p \int_0^\infty p(S) \, (\dfrac{S}{A})^b \, dS$
Total Damage	Cumulative fatigue over service time T	$D_{\text{total}} = \nu_p T \int_0^\infty p(S) \, (\dfrac{S}{A})^b \, dS$
Life Assessment	Pass/fail and remaining life	$D_{\text{total}} \leq 1 \Rightarrow$ Safe; $\quad T_{\text{remaining}} = \dfrac{1}{\dot{D}}$

6 Application Domains

Frequency-domain spectral methods have been developed and refined over decades to address fatigue assessment challenges in diverse engineering domains, each with distinct loading characteristics, operational environments, and regulatory requirements. While the Dirlik [13] method is often considered the most robust general-purpose approach, empirical evidence and practical experience have shown that alternative methods (Tovo-Benasciutti [7], Zhao-Baker [6], narrowband-based approaches [61]) may be better suited for specific application contexts. This section synthesizes domain-specific knowledge about where each method excels, explaining the physical reasons for their superiority in particular applications [71].

6.1 Aerospace Applications

Aerospace structures (fixed-wing aircraft, helicopters, spacecraft, airborne equipment) experience narrowband to moderately narrowband random vibration loading dominated by aerodynamic and engine-induced excitation. The flight environments typically activate one or two primary structural modes with concentrated energy around resonant frequencies, particularly in the frequency range 5–500 Hz [72, 73].

In this domain, the signal has a relatively narrow bandwidth, characterized by the parameter $\alpha_2 \approx 0.7 - 0.95$. This is observed with energy concentrated near specific resonant modes. It is generally considered that aeronautic white noise is a random process, this is observed by the stationarity (or near stationarity) of the signal during steady-state flight.

For typical aerospace narrowband vibration environments, both Dirlik and the classical narrowband approximation (Rice, Miles, Bendat) perform well [72]. However:

- Dirlik remains the gold standard due to its robustness across varying bandwidth conditions and its universal adoption in commercial aerospace finite element platforms.
- The narrowband approximation, while sometimes overly conservative, is acceptable and often preferred for safety-critical components because is naturally provides conservative estimates. For narrowband processes where $\alpha_2 > 0.85$, narrowband predictions are quite accurate [73].

For helicopter structures or aircraft experiencing multimodal excitation (rotor-induced vibration, blade flutter, shock absorber dynamics), the Tovo-Benasciutti method provides excellent accuracy without additional computational complexity [72].

The physical reasoning behind those choices is that the aerospace domain's preference for narrowband-based methods stems from the physics of structural dynamics. Aircraft and helicopter structures are designed with

well-separated natural frequencies and significant modal damping (typically 2–5% critical damping). When subjected to broadband aerodynamic noise or engine vibration, only resonant modes are efficiently excited, concentrating the response energy in narrow frequency bands. This concentrated energy creates a stress history that is nearly sinusoidal with slowly modulated amplitude—exactly the scenario where narrowband and Dirlik methods excel [74].

Aerospace certification relies heavily on standards including MIL-STD-810G, FAA AC 23.305, and industry guidelines. These standards typically specify narrowband or semi-empirical methods for random vibration fatigue prediction, though Dirlik is increasingly accepted. Experimental validation through ground vibration tests (GVT) and flight tests is required to verify analytical predictions [72, 75].

6.2 Automotive Applications

Ground vehicles experience broadband to extremely broadband random vibration from tire-road interaction, engine vibration, and suspension dynamics. The vibration profiles feature:

- Very broad spectral bandwidth ($\alpha_2 \approx 0.1 - 0.4$), with energy spread across 10 Hz to 2000 Hz.
- Multiple resonant modes activated simultaneously (suspension modes, body modes, component-specific resonances).
- Complex acceleration profiles with multiple peaks, valleys, and wideband noise.

Extensive automotive-focused research has demonstrated that the enhanced ZHao-Baker method (ZB2) is the most accurate for typical automotive accelerated vibration test profiles [12, 76]. ZB2 has been specifically tuned through Monte Carlo simulations on automotive-industry test spectra (multi-peak profiles with broad bandwidth), and it provides consistently conservative estimates (safe-side predictions), which is critical for component durability certification. Studies [12, 71] comparing multiple methods on real automotive test profiles found ZB2 to be the only method providing conservative damage estimates across diverse road conditions and component types. Finally, given its mathematical definition given in Equation 34 is handles complex interactions between multiple spectral models without oversimplification.

For general automotive applications less demanding than accelerated testing, Tovo-Benasciutti and Dirlik provide adequate accuracy. However, for critical durability programs, ZB2 is preferred because of its superior match to rainflow-counted reference damage [71].

The physical interpretation behid these choices lies in the fact that automotive environments create wideband spectra because ground excitation (potholes, rough pavement, ripple patterns) contains significant energy across a broad frequency range. Multiple structural modes—suspension, chassis, powertrain—contribute simultaneously, creating a complex stress distribution with both large and small stress cycles interspersed. Wideband methods like ZB2 capture this complexity by using higher-order spectral moments (m_2, m_4) to detect and properly weight the interaction between modes. The ZB2 method's empirical calibration specifically targeted automotive test profiles, where the energy distribution and cycle interactions are markedly different from aerospace or marine environments [76].

Automotive fatigue testing follows standards including ISO 16750-3 (Environmental Conditions for Vehicle Components), SAE J1211 (Test Procedures for Random Vibration) [77], and company-specific OEM protocols (Volkswagen, Ford, General Motors, etc.). These standards now increasingly accept frequency-domain methods, and many recognize the Zhao-Baker method as the preferred choice for automotive accelerated testing [78].

6.3 Industrial Machinery and Rotating Equipment

Rotating machinery (compressors, pumps, turbines, motors) and their structural supports experience narrowband forcing from discrete rotating frequencies (1x, 2x, 3x shaft speed, etc.). They also experience broadband random excitation from turbulence (compressor surge, cavitation in pumps), and mixed spectra combining deterministic harmonics with random broadband background [79, 80].

The primary recommendation present in the literature is the use of the Narrowband approximation method or the Dirlik. The selection of the method depends on the degree of randomness of the signal. In fact, for

machines with strong deterministic forcing and minimal random broadband content, the narrowband approximation method is acceptable. However, for machines with significant turbulent excitation or cavitation (creating broadband), Dirlik is preferred.

For many industrial applications, testing combines deterministic with random excitation. Specialized combined methods of hybrid time-domain/frequency-domain approaches may be needed [78].

6.4 Offshore and Wind Energy Application

Offshore structures (oil platforms, floating systems, wind turbines) experience multimodal, non-stationary random loading from wave excitation, wind loading, structural modes, and combined wave-wind effects. The resulting tower stress PSD is typically multimodal with very broad bandwidth ($\alpha_2 < 0.2$ common), presenting a challenge for simple spectral methods [81–83].

For offshore structures, Dirlik combined with modal superposition is the standard approach. However, recent research has identified specific refinements [58, 83]:

- Pure Dirlik works well for broadband combined spectra, that is, considering the entire signal without decomposing it.
- For highly multimodal cases (wind + wave + structural modes), using separate Dirlik calculations for each mode and summing the damage improves accuracy.

The second recommended method is the Tovo-Benasciutti method. In fact, once the wind and wave inputs are combined into a total stress spectrum, this method provides and alternative check and is often equally accurate [83].

For structures with exactly three dominant modes (wind, primary wave, secondary wave), the Gao-Moan method was specifically designed for this case and can provide excellent accuracy, though Dirlik is usually simpler to implement [84].

This comes from the fact that offshore structures present a unique challenge because the loading is inherently multimodal: wind and wave excitations activate different structural modes, and the waves themselves contain multiple frequency components. Dirlik's three-component distribution model (exponential + two Rayleigh components) is well-suited to capture this complexity. The method's flexibility in decomposing the stress distribution into multiple mode contributions makes it particularly robust for broad, complex offshore spectra [81].

Additionally, offshore fatigue is often long-term damage assessment, requiring integration over many operational sea states with different ocean and meteorological conditions (wind speed, wave height, direction). The efficiency of spectral methods (vs. time-domain rainflow) becomes critical—Dirlik allows rapid evaluation of hundreds of sea states, making design optimization and reliability analysis tractable [58, 83].

Offshore fatigue design follows DNV GL-RP-C203 (Recommended Practice for Fatigue Design) [85], API RP 2A (Recommended Practice for Planning, Designing, and Constructing Fixed Offshore Platforms) [86], and IEC 61400-1 (Wind Turbine Safety) [87]. These standards recognize frequency-domain methods and often mandate Dirlik for environmental loading analysis.

7 Conclusion

This paper has provided a comprehensive and structured review of the principal methods used to estimate fatigue damage under random vibration loading in the frequency domain. Traditional time-domain rainflow counting methods remain the reference for fatigue analysis, but their computational cost and dependence on long-duration time histories make them impractical for many real-world engineering applications. In contrast, frequency-domain techniques offer a powerful alternative framework that leverages spectral information to achieve efficient and reliable fatigue estimates, particularly for Gaussian and stationary processes.

A critical examination of the available probability-distribution models—beginning with the classical narrow-band approximation of Rice and Miles and extending through modern wide-band corrections such as Wirsching–Light,

$\alpha_{0.75}$, Zhao–Baker, and Gao–Moan—highlights the substantial progress made in overcoming the limitations of early approaches. Among these, the Tovo–Benasciutti, Zhao-Baker and Dirlik formulations continue to emerge as the most accurate and widely used for broadband signals, while the Narrowband approximation and correction methods are appropriate for narrowband signals.

Beyond the mathematical models, this review also presented a practical framework for applying spectral methods in engineering workflows, from raw vibration measurement through FRF-based stress reconstruction, PSD characterization, material modeling, and damage accumulation using Miner's rule. The framework illustrates that, when carefully implemented, spectral methods can deliver dependable fatigue-life predictions with significant computational advantages compared to time-domain techniques.

Despite their strengths, frequency-domain methods are not without limitations. Many rely on assumptions of Gaussianity, stationarity, and uniaxial loading, and their performance may degrade in the presence of non-Gaussian processes, transient phenomena, or strong nonlinearities. Moreover, most existing methods rely on empirical approximations rather than closed-form physical derivations, leaving room for further theoretical refinement. These challenges highlight ongoing opportunities for research, including improved modeling of multimodal and non-Gaussian spectra, hybrid time–frequency approaches, and data-driven enhancements leveraging machine learning.

Overall, frequency-domain fatigue methods constitute a mature, practical, and computationally efficient toolbox that is highly relevant for contemporary applications ranging from aerospace and automotive structures to industrial machinery and offshore wind systems. By synthesizing the developments in this field and clarifying the assumptions, advantages, and limitations of each method, this review provides a foundation for informed methodological choices and serves as a reference point for ongoing and future work in vibration-fatigue analysis—particularly within the broader context of this PhD research.

References

[1]I. Rychlik, "Fatigue and Stochastic Loads", Scandinavian Journal of Statistics **23**, 387–404 (1996).

[2]M. Matsuishi and T. Endo, "Fatigue of metals subjected to varying stress", Japan society of mechanical engineers, Fukuoka, Japan **68**, 37–40 (1968).

[3]A. Palmgren, "Die lev/bensdauer von kugellagern", VDI. Z. **68**, 339–341 (1924).

[4]M. A. Miner, "Cumulative damage in fatigue", (1945).

[5]A. Halfpenny, "A Frequency Domain Approach for Fatigue Life Estimation from Finite Element Analysis", Key Engineering Materials **167–168**, 401–410 (1999).

[6]W. Zhao and M. J. Baker, "On the probability density function of rainflow stress range for stationary Gaussian processes", International Journal of Fatigue **14**, 121–135 (1992).

[7]R. Tovo, "Cycle distribution and fatigue damage under broad-band random loading", International Journal of Fatigue **24**, 1137–1147 (2002).

[8]G. Petrucci and B. Zuccarello, "Fatigue life prediction under wide band random loading", Fatigue & Fracture of Engineering Materials & Structures **27**, 1183–1195 (2004).

[9]I. Rychlik, "A new definition of the rainflow cycle counting method", International Journal of Fatigue **9**, 119–121 (1987).

[10]J. M. Elson and J. M. Bennett, "Calculation of the power spectral density from surface profile data", Applied optics **34**, 201–208 (1995).

[11]*On the estimation of the fatigue cycle distribution from spectral density data - G Petrucci, B Zuccarello, 1999*, https://journals.sagepub.com/doi/abs/10.1243/0954406991522437.

[12]M. Mršnik et al., "Frequency-domain methods for a vibration-fatigue-life estimation – Application to real data", International Journal of Fatigue **47**, 8–17 (2013).

[13]T. Dirlik, "Application of computers in fatigue analysis", PhD thesis (University of Warwick, Jan. 1985).

[14]Z. Gao and T. Moan, "Frequency-domain fatigue analysis of wide-band stationary Gaussian processes using a trimodal spectral formulation", International Journal of Fatigue **30**, 1944–1955 (2008).

[15]D. Benasciutti and R. Tovo, "Rainflow cycle distribution and fatigue damage in gaussian random loadings", Report of engineering department. University of Ferrara (Italy) (2004).

[16]P. H. Wirsching and M. C. Light, "Fatigue under wide band random stresses", Journal of the Structural Division **106**, 1593–1607 (1980).

[17]D. Benasciutti, "Fatigue analysis of random loadings (phd thesis)", University of Ferrara (2004).

[18]D. Benasciutti and R. Tovo, "Spectral methods for lifetime prediction under wide-band stationary random processes", International Journal of fatigue **27**, 867–877 (2005).

[19]T. Łagoda et al., "Fatigue life calculation by means of the cycle counting and spectral methods under multiaxial random loading", Fatigue & Fracture of Engineering Materials & Structures **28**, 409–420 (2005).

[20]K. Shin and J. Hammond, *Fundamentals of Signal Processing for Sound and Vibration Engineers* (John Wiley & Sons, Apr. 2008).

[21]D. E. Newland, "An introduction to random vibrations and spectral analysis", (No Title) (1984).

[22]U. Lee and J. Shin, "A frequency response function-based structural damage identification method", Computers & Structures **80**, 117–132 (2002).

[23]R. N. Bracewell, "The Fourier Transform", Scientific American **260**, 86–95 (1989).

[24]N. W. Bishop, "The use of frequency domain parameters to predict structural fatigue", PhD thesis (University of Warwick, 1988).

[25]N. M. M. Maia and J. M. (M. Montalvão e Silva, *Theoretical and experimental modal analysis*, Mechanical Engineering Research Studies (Research Studies Press and Wiley, 1997).

[26]R. R. Craig Jr and A. J. Kurdila, *Fundamentals of structural dynamics* (John Wiley & Sons, 2006).

[27]M. Tarpø et al., "Operational modal analysis based prediction of actual stress in an offshore structural model", Procedia Engineering, X International Conference on Structural Dynamics, EURODYN 2017 **199**, 2262–2267 (2017).

[28]D. J. Inman, *Engineering vibration*, Fifth edition (Pearson, Hoboken, NJ, 2022).

[29]M. Zóltowski, R. Martinod, et al., "Technical condition assessment of masonry structural components using frequency response function (frf)", Masonry International (2016).

[30]F. J. Fahy, "Measurement of acoustic intensity using the cross-spectral density of two microphone signals", The Journal of the Acoustical Society of America **62**, 1057–1059 (1977).

[31]D. J. MacKay et al., "Introduction to gaussian processes", NATO ASI series F computer and systems sciences **168**, 133–166 (1998).

[32]E. H. Vanmarcke, "Properties of spectral moments with applications to random vibration", Journal of the Engineering Mechanics Division **98**, 425–446 (1972).

[33]M. Muñiz-Calvente et al., "A comparative review of time-and frequency-domain methods for fatigue damage assessment", International Journal of Fatigue **163**, 107069 (2022).

[34]C. M. Sonsino, "Course of SN-curves especially in the high-cycle fatigue regime with regard to component design and safety", International Journal of Fatigue **29**, 2246–2258 (2007).

[35]N. Dowling, "Fatigue life prediction for complex load versus time histories", Journal of Engineering Materials and Technology **105**, 206–214 (1983).

[36]A. J. Hallinan Jr, "A review of the weibull distribution", Journal of quality technology **25**, 85–93 (1993).

[37]W. Schütz, "A history of fatigue", Engineering fracture mechanics **54**, 263–300 (1996).

[38]O. BASQUIN, *The exponential law of endurance tests american society for testing and materials, 1910.*

[39]J. Kohout and S. Ve˘chet, "A new function for fatigue curves characterization and its multiple merits", International Journal of Fatigue **23**, 175–183 (2001).

[40]R. Nijssen, "Phenomenological fatigue analysis and life modelling, fatigue life prediction of composites and composite structures, ed. by anastasios p", Vassilopoulos, Woodhead Publ. Ltd and CRC Press LLC (2010).

[41]J. J. Xiong and R. A. Shenoi, *Fatigue and Fracture Reliability Engineering* (Springer Science & Business Media, Jan. 2011).

[42]I. Burhan and H. S. Kim, "Sn curve models for composite materials characterisation: an evaluative review", Journal of Composites Science **2**, 38 (2018).

[43]C. Stromeyer, "The determination of fatigue limits under alternating stress conditions", Proceedings of the Royal Society of London. Series A, Containing Papers of a Mathematical and Physical Character **90**, 411–425 (1914).

[44]J. Spindel and E. Haibach, "Shape of s-n curves", Statistical analysis of fatigue data **744**, 89 (1981).

[45]F. Stüssi, *Die theorie des dauerfestigkeit und die versuche von august wöhler* (Verlag VSB, 1955).

[46]F. Bastenaire, *New method for the statistical evaluation of constant stress amplitude fatigue-test results* (ASTM International, 1972).

[47]E. Castillo et al., "Statistical model for fatigue analysis of wires, strands and cables", in Iabse proceedings (1985), pp. 1–40.

[48]V. V. Bolotin, *Mechanics of fatigue* (Crc Press, 2020).

[49]F. G. Pascual and W. Q. Meeker, "Estimating fatigue curves with the random fatigue-limit model", Technometrics **41**, 277–289 (1999).

[50]P. Strzelecki et al., "Estimation of fatigue S-N curves for aluminium based on tensile strength – proposed method", MATEC Web Conf. **338**, 01026 (2021).

[51]M. T. Todinov, "Necessary and sufficient condition for additivity in the sense of the Palmgren–Miner rule", Computational Materials Science **21**, 101–110 (2001).

[52]K. Hectors and W. De Waele, "Cumulative Damage and Life Prediction Models for High-Cycle Fatigue of Metals: A Review", Metals **11**, 204 (2021).

[53]K. A. Zakaria et al., "A review of the loading sequence effects on the fatigue life behaviour of metallic materials", Journal of Engineering Science and Technology Review **9**, 189–200 (2024).

[54]B.-T. Huang et al., "Fatigue Deformation Model of Plain and Fiber-Reinforced Concrete Based on Weibull Function", Journal of Structural Engineering **145**, 04018234 (2019).

[55]S. S. Manson and G. R. Halford, *Fatigue and durability of metals at high temperatures* (ASM International, 2009).

[56]J. Zhang et al., "Study on Damage Accumulation and Life Prediction with Loads below Fatigue Limit Based on a Modified Nonlinear Model", Materials (Basel) **11**, 2298 (2018).

[57]C. Lalanne, *Mechanical vibration and shock analysis, fatigue damage*, Vol. 4 (John Wiley & Sons, 2014).

[58]T. Dirlik and D. Benasciutti, "Dirlik and Tovo-Benasciutti Spectral Methods in Vibration Fatigue: A Review with a Historical Perspective", Metals **11**, 1333 (2021).

[59]S. O. Rice, "Mathematical analysis of random noise", The Bell System Technical Journal **23**, 282–332 (1944).

[60]J. S. Bendat, "PROBABILITY FUNCTIONS FOR RANDOM RESPONSES: PREDICTION O F PEAKS, FATIGUE DAMAGE, AND CATASTROPHIC FAILURES",

[61]J. W. MILES, "On Structural Fatigue Under Random Loading", Journal of the Aeronautical Sciences **21**, 753–762 (1954).

[62]G. Jiao and T. Moan, "Probabilistic analysis of fatigue due to gaussian load processes", Probabilistic Engineering Mechanics **5**, 76–83 (1990).

[63]C. E. Larsen and T. Irvine, "A Review of Spectral Methods for Variable Amplitude Fatigue Prediction and New Results", Procedia Engineering **101**, 243–250 (2015).

[64]S. Jun and J.-B. Park, "Development of Empirical Formulas for Approximate Spectral Moment Based on Rain-Flow Counting Stress-Range Distribution", J. Ocean Eng. Technol. **35**, 257–265 (2021).

[65]S. Sakai and H. Okamura, "On the distribution of rainflow range for gaussian random processes with bimodal psd", JSME international journal. Ser. A, Mechanics and material engineering **38**, 440–445 (1995).

[66]T.-T. Fu and D. Cebon, "Predicting fatigue lives for bi-modal stress spectral densities", International Journal of Fatigue **22**, 11–21 (2000).

[67]J. Goodman, *Mechanics applied to engineering* (Longmans, Green, 1919).

[68]A. Kaľavský et al., "Influence of PSD Estimation Parameters on Fatigue Life Prediction in Spectral Method", Materials (Basel) **16**, 1007 (2023).

[69]A. Zorman et al., "Vibration fatigue by spectral methods—a review with open-source support", Mechanical systems and signal processing **190**, 110149 (2023).

[70]A. Niesłony et al., "The use of spectral method for fatigue life assessment for non-gaussian random loads", acta mechanica et automatica **10**, 100–103 (2016).

[71]M. Mršnik et al., "Vibration fatigue using modal decomposition", Mechanical Systems and Signal Processing **98**, 548–556 (2018).

[72]E. Habtour et al., "Review of response and damage of linear and nonlinear systems under multiaxial vibration", Shock and Vibration **2014**, 294271 (2014).

[73]M. Wang, "Numerical analysis of random vibration fatigue for a typical airborne equipment", Vibroengineering Procedia **49**, 233–238 (2023).

[74]M. Wang, "Numerical analysis of random vibration fatigue for a typical airborne equipment", Vibroengineering PROCEDIA **49**, 233–238 (2023).

[75]U. Tekeci and B. Yıldırım, "Predicting fatigue life of a mount of a device with shock absorber", Politeknik Dergisi **27**, 1005–1015 (2024).

[76]Y. S. Kong et al., "Vibration fatigue analysis of carbon steel coil spring under various road excitations", Metals **8**, 617 (2018).

[77]H. Su, "Vibration test specification for automotive products based on measured vehicle load data", SAE Transactions, 571–581 (2006).

[78]C.-J. Kim, "Accelerated sine-on-random vibration test method of ground vehicle components over conventional single mode excitation", Applied Sciences **7**, 805 (2017).

[79]I. Bagri et al., "Vibration Signal Analysis for Intelligent Rotating Machinery Diagnosis and Prognosis: A Comprehensive Systematic Literature Review", Vibration **7**, 1013–1062 (2024).

[80]S. Maurya and N. K. Verma, "On Designing Features for Condition Monitoring of Rotating Machines",

[81]J. A. Ribeiro et al., "Offshore wind turbine tower design and optimization: a review and ai-driven future directions", Applied Energy **397**, 126294 (2025).

[82]A. Chehouri et al., *Wind turbine design: multi-objective optimization* (InTech, 2016).

[83]D. P. Liu et al., "On long-term fatigue damage estimation for a floating offshore wind turbine using a surrogate model", Renewable Energy **225**, 120238 (2024).

[84]J. Xu et al., "Research on the scope of spectral width parameter of frequency domain methods in random fatigue", Applied Sciences **10**, 4715 (2020).

[85]I. Lotsberg, "Background for revision of dnv-rp-c203 fatigue analysis of offshore steel structure", in International conference on offshore mechanics and arctic engineering, Vol. 41979 (2005), pp. 297–306.

[86]API., *Api 2a-wsd: recommended practice for planning, designing and constructing fixed offshore platforms-working stress design* (American Petroleum Institute, 2000).

[87]P. H. Madsen and D. Risø, "I ntroduction to the i ec 61400-1 standard", (2008).